(3) de Gennes, P.-G. *J. Phys.* (*Les Ulis, F.*) **1975**, *36*, L-55.
(4) Sanchez, I. C. *Macromolecules* **1979**, *12*, 980.
(5) Mazur, J.; McCrackin, F. L.; *J. Chem. Phys.* **1968**, *49*, 648.
(6) McCrackin, F. L.; Mazur, J.; Guttman, C. M. *Macromolcules* **1973**, *6*, 859.
(7) Domb, C. *Polymer* **1974**, *15*, 259.
(8) Rapaport, D. C. *Macromolecules* **1974**, *7*, 64 *J. Phys. A.: Math. Gen.* **1977**, *10*, 637.
(9) de Gennes, P.-G. *Phys. Lett. A.* **1972**, *38*, 339.
(10) des Cloiseaux, J. *J. Phys.* (*Les Ulis, Fr.*) **1975**, *36*, 281.
(11) de Gennes, P.-G. "Scaling Concepts in Polymer Physics"; Cornell University Press: Ithaca, NY, 1979.
(12) Kholodenko, A. L.; Freed, K. F. *J. Chem. Phys.* **1984**, *80*, 900.
(13) Cuniberti, C.; Bianchi, U. *Polymer* **1974**, *15*, 346.
(14) Slagowski, E.; Tsai, B.; McIntyre, D. *Macromolecules* **1976**, *9*, 687.
(15) Nierlich, M.; Cotton, J. P.; Farnoux, B. *J. Chem. Phys.* **1978**, *69*, 1379.
(16) Swislow, G.; Sun, S. T.; Nishio, I.; Tanaka, T. *Phys. Rev. Lett.* **1980**, *44*, 796.
(17) Bauer, D. R.; Ullman, R. R. *Macromolecules* **1980**, *13*, 392.
(18) Sun, S. T.; Nishio, I.; Swislow, G.; Tanaka, T. *J. Chem. Phys.* **1980**, *73*, 5971.
(19) Williams, C.; Brochard, F.; Frisch, H. L. *Annu. Rev. Phys. Chem.* **1981**, *32*, 433.
(20) Martins, A. F.; Ferreira, J. B.; Volino, F.; Blumstein, A.; Blumstein, R. B. *Macromolecules* **1983**, *16*, 279.
(21) Blumstein, A.; Thomas, O. *Macromolecules* **1982**, *15*, 1264.
(22) Krigbaum, W. R.; Watanabe, J.; Ishikawa, T. *Macromolecules* **1983**, *16*, 1271.
(23) DiMarzio, E. A.; Macromolecules **1984**, *17*, 969.
(24) DiMarzio, E. A.; *J. Chem. Phys.* **1961**, *35*, 658.
(25) Wulf, A.; DeRocco, A. G.; *J. Chem. Phys.* **1971**, *55*, 12.
(26) Grosberg, A. Yu.; Khokhlov, A. R. *Adv. Polym. Sci.* **1981**, *41*, 53.
(27) Grosberg, A. Yu.; Khokhlov, A. R. "Problems in Solid State Physics"; Prokhorov, A. M., Prokhorov, A. S., Eds.; Mir: Moscow, 1984 (in English); p 330.
(28) Onsager, L. *Ann. N.Y. Acad. Sci.* **1949**, *51*, 627.
(29) Flory, P. J. *Proc. R. Soc. London* **1956**, *234*, 60.
(30) Boehm, R. E.; Martire, D. E.; Armstrong, D. W.; Bui, K. H. *Macromolecules* **1983**, *16*, 466.
(31) Apart from an unimportant bond orientational degeneracy factor $M!/((M/3)!)^3 \simeq 3^M$.
(32) In general $Q(\beta, L) = \sum_V \sum_S Q(\beta, L, \mathbf{V}, \mathbf{S})$. However, utilization of the maximum term approximation to $Q$ or ln $Q$ is anticipated by considering that the only important contribution to the sum comes from the term evaluated at the volume $V$ and order parameter $S$ that maximize $Q$.
(33) Post, C. B.; Zimm, B. H. *Biopolymers* **1979**, *18*, 1487, 1495.
(34) Berne, B. J.; Pecora, R. "Dynamic Light Scattering"; Wiley-Interscience: New York, 1976; Chapters 7 and 8.
(35) Lakowicz, "Principles of Fluorescence Spectroscopy"; Plenum Press: New York, 1983; Chapters 5 and 6.
(36) Lerman, Cold Spring Harbor Symposium on Quantitative Biology, **1973**, Vol, XXXVIII, 59.
(37) Dayantis, J. *Makromol. Chem., Rapid Commun.* **1984**, *5*, 71.
(38) Vasilenko, S. V.; Khokhlov, A. R.; Shibaev, V. P. *Macromolecules* **184**, *17*, 2270.
(39) Tanaka, T.; Hocher, L.; Benedek, G. *J. Chem. Phys.* **1973**, *59*, 5151.
(40) Tanaka, T.; Ishiwata, S.; Ischimoto, C. *Phys. Rev. Lett.* **1977**, *58*, 771.
(41) Brochard, F. *J. Phys.* (*Les Ulis, Fr.*) **1979**, *40*, 1049.
(42) Boehm, R. E.; Martire, D. E. *Mol. Phys.* **1979**, **38**, 1973.
(43) Boehm, R. E.; Martire, D. E. *Mol. Phys.* **1978**, *36*, 1.

# Novel Approach for the Processing of Thermotropic Liquid-Crystal Polymers. 1. Thermodynamics and Solid-State Transesterification

**Eric R. George and Roger S. Porter***

*Materials Research Laboratory, Polymer Science and Engineering Department, University of Massachusetts, Amherst, Massachusetts 01003.* *Received April 15, 1985*

ABSTRACT: The phase diagram has been obtained for poly(bisphenol E isophthalate-*co*-naphthalate) in a para-substituted phenyl ester of terephthalic acid, bis(*p*-(methoxycarbonyl)phenyl) terephthalate. This binary system exhibits miscibility in a nematic phase and does not form cocrystals. The crystal-to-nematic phase transition has been characterized by the temperature and heat of transition data and by the Flory–Huggins theory for the melting point depression of a polymer–diluent system. From the extrapolated melting point depression data, the heat of fusion of the crystal–nematic phase transition for the polyester is found to be 20.3 ± 0.6 cal/g. The eutectic composition is ~24 wt % polymer at 247 °C with a eutectic heat of transition of ~20 cal/g. The heat of fusion of bis(*p*-(methoxycarbonyl)phenyl) terephthalate is ~30.0 cal/g for the crystal–nematic phase transition. The phase behavior was examined at high copolyester content with three different molecular weights of BPE/I/N20. These blends were subsequently transesterified in the solid state at 220 °C, and the changes in phase transitions are reported. The phase behavior and transesterification were characterized by DSC, TGA, polarized light microscopy, X-ray diffraction, and dilute-solution viscometry. The thermodynamic criteria for the melting point depression and the kinetics of transesterification are also reported for the utilization of this new processing technique.

## Introduction

**Background.** The fundamental investigation and potential industrial use of thermotropic liquid crystal polymers (TLCP) are beset by difficulties. These rigid extended chain structures have a high axial ratio and a low entropy of "melting" (transition to the liquid-crystal phase). This puts the transition from the semicrystalline to liquid-crystal phase above temperatures for significant thermal and/or oxidative degradation. However, rigid extended chain, wholly aromatic structures are required for enhanced mechanical properties, particularly high-tensile moduli.

An approach for lowering the crystal–mesophase temperatures of these aromatic polyesters is via the incorporation of asymmetric units, kinks, and flexible bonds.[1] These additions to the original rigid TLCP may disrupt crystalline order and increase the number of possible conformations in the liquid-crystal state and lower the

0024-9297/86/2219-0097$01.50/0 

temperature of the crystal–mesophase transition.

In a previous paper,[2] we disclosed a route for the preparation of TLCP utilizing a eutectic-type phase diagram of a TLCP with a bifunctional dimethyl ester liquid crystal (DMELC). The technique features the formation of a lowered crystal–mesophase transition and a lower viscosity for blends than for the pure polymer. This state is followed by the incorporation of the DMELC into the TLCP main chain via solid-state transesterification at 220 °C.

The copolyester under investigation, poly(bisphenol E isophthalate-*co*-naphthalate) (BPE/I/N20), contains 40 mol % isophthalate units, a high fraction for TLCP. The meta substitution is a "kink" in the extended chain, aromatic structure. Data obtained by rheology, birefringence, X-ray diffraction, thermal analysis, and miscibility studies[2-4] are consistent with a nematic phase above 284 °C. Extrudates did not exhibit high-tensile moduli, presumably due to the isophthalate content and the fact that the extrudate was neither drawn under tension, quenched, nor heat-treated.

The all-para-substituted DMELC that was synthesized and characterized offers the following advantages for

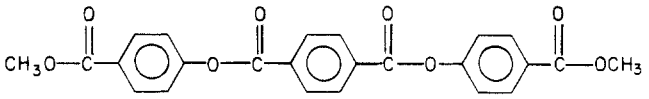

DMELC

blending with and subsequent reaction with a TLCP:[2] a nematic mesophase above 254 °C which can co-mesophase with a TLCP; bifunctionality with the potential for solid-state transesterification; and para substitution, which after incorporation into a TLCP would contribute to enhanced rigidity of the chain.

A two-phase crystalline mixture followed on heating by a transition into a mixed miscible liquid or liquid-crystal phase are the basic criteria for eutectic-type behavior. The depression of the crystal–mesophase transition for the polymer should be possible for a range of TLCP. This procedure may thus represent a general concept for thermotropic polymers.

The key disadvantage of DMELC is that it contains a nonstoichiometric equivalent of acid to hydroxyl functionality. The molecular weight of the polymer thus cannot exceed that of the original polymer and in fact must be less. The reactions of these binary blends were characterized as a function of initial molecular weight, reaction time, and concentration.

**Eutectic Phase Diagrams in Binary Nematic Mesophase Systems of Low Molecular Weight.** For low molecular weight liquid crystals the thermodynamics of ideal solutions often predict well the melting transition curves for the crystal–nematic phase transition over the compositional phase diagram.[5-8] The conditions for ideality include the following: the components do not cocrystallize; the components do not react; the components are miscible across the entire phase diagram in the nematic phase; and the heat of mixing $\simeq 0$ in the mesophase.

The occurrence of cocrystals is likely in neighboring members of an homologous series, causing a measurable difference between experimental and predicted phase diagrams. The similarity of structure favors miscibility in the nematic phase, yet increases the possibility of cocrystallization. A model system of an ideal eutectic is illustrated by the binary-phase behavior of the system *p*-azoxyanisole–*p*-azoxyphenetole.[5] The phase diagram and the associated heat of transition data are in Figures 1 and 2, respectively. Figure 1 illustrates the eutectic point as the intersection of the transition temperatures of the

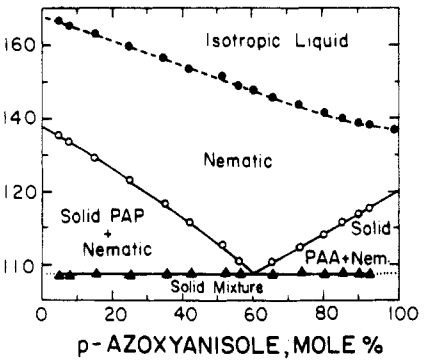


**Figure 1.** Phase diagram of *p*-azoxyanisole–*p*-azoxyphenetole system.

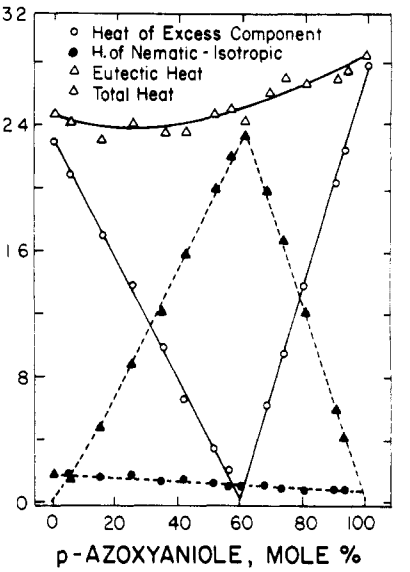


**Figure 2.** Transition heats of *p*-azoxyanisole–*p*-azoxyphenetole system.

excess components, while the heat of transition for the excess component tends to 0 at the eutectic.

The melting point depression for ideal systems can be determined via the van't Hoff equation

$$\frac{1}{T_m} - \frac{1}{T_{m_0}} = -\frac{R}{\Delta H_2} \ln N_2 \qquad (1)$$

where $T_m$ is the melting temperature of the excess component for a solute mole fraction $N_2$, $T_{m_0}$, is the melting point of the pure excess component, $R$ is the gas constant ($\sim$1.987 cal/(mol·K)), and $\Delta H_2$ is the heat of fusion of the pure excess component. The slope of the melting point depression is inversely proportional to the heat of fusion $\Delta H_2$. Thus, if the two pure components have a similar $\Delta H_2$ and $T_{m_0}$ and are approximately the same molecular weight, the eutectic point will approach $\sim$50 mol %. Note that the only compositions which exhibit a single transition from the crystal to the nematic phase are the pure components and the eutectic composition.

The effect of metathetical reactions on the phase diagram of Schiff base liquid crystals has been investigated by Albert.[9] These exchange reactions convert the two-component system into a four-component system, and a broad minimum is observed instead of a eutectic point for many systems. The metathetic reaction is an example of nonideality that will modify a eutectic phase diagram.

**Eutectic Phase Diagrams in Binary Polymer–Diluent Systems.** Phase studies of TLCP with low molecular weight liquid crystals have been studied for several

systems.[10-16] The binary blends have been prepared by melt mixing and by solvent casting. The thermal history of the blends varied for each study, which could lead to differences in subsequent thermal transitions on heating. Nonideal solution behavior was convirmed for each phase diagram, since none followed the depression of the phase transition predicted by the van't Hoff equation.

Polymer–diluent systems are never in thermodynamic equilibrium since the polymer is only partially crystalline and contains a distribution of molecular weight. The long-chain nature of the polymer affects primary and eutectic crystallization. In fact, the eutectic crystallization or melting is often not observed in polymer–diluent systems, particularly at high polymer concentration.[10,13-15,20-24] The eutectic phase boundary represents a separation of two two-phase regions (except at the eutectic point itself). In a binary blend at equilibrium this phase boundary is expected to be a horizontal straight line.

The Flory–Huggins (F–H) theory for the free energy change ($\Delta G_m$) on mixing of a polymer–diluent system has been successfully applied for many systems.[17] The nonideality of mixing may be represented by a Scatchard–Hildebrand[18,19] type of mixing enthalpy and the entropy of mixing derived by the Flory–Huggins lattice model. For high molecular weight polymers the resulting expression for melting point depression becomes

$$\frac{1}{T_m} - \frac{1}{T_m^\circ} = \left(\frac{R}{\Delta H_u}\right)\left(\frac{V_u}{V_1}\right)(\phi_1 - \chi_1\phi_1^2) \qquad (2)$$

where $T_m$ is the melting point of the polymer as the excess component, $\phi_1$ is the volume fraction of diluent, $T_m^\circ$ is the melting point of the theoretical polymer perfect crystal, $R$ is the gas constant, $V_u$ is the molar volume of the polymer repeat unit, $V_1$ is the molar volume of the diluent, and $\chi_1$ is the Flory interaction parameter. Analagous to ideal solutions, the slope of the melting point depression should be inversely proportional to $\Delta H_u$ with curvature indicative of the magnitude of $\chi_1$.[17] A plot of $(1/T_m - 1/T_{m_0})/\phi_1$ vs. $\phi_1$ yields as an intercept $(R/\Delta H_u)(V_u/V_1)$, and the excess enthalpy of interaction may be computed from the slope, $(R/\Delta H_u)(V_u/V_1)\chi_1$.

Equation 2 contains two adjustable parameters both of which are dependent on the morphology of the polymer. $T_{m_0}$ can be estimated by extrapolation methods.[24] The technique involves annealing at temperatures approaching $T_{m_0}$, but polyesters will often react at these temperatures. The second parameter, $V_u/V_1$, the ratio of specific molar volume of the polymer repeat unit and the diluent, is calculated from the density of the amorphous liquids. $V_u$ may be estimated from the density of a quenched amorphous polymer.

Studies of eutectic phase diagrams of polymer–crystalline diluent systems, with an emphasis on the crystalline morphology of the eutectic composition, have been reported.[20-23] Wunderlich[24] discussed the F–H theory as applied to crystalline diluents; many examples were cited that exhibit close agreement with eq 2. The melting temperature of the excess polymer component was shown to be dependent on crystallization temperature and the heating rates at which the DSC thermograms were recorded.

The temperature of crystallization affects the degree of crystallinity as well as the crystalline perfection of the polymer. Equation 2 shows that the melting point depression depends on the heat of fusion per repeat unit $\Delta H_u$ of the polymer. The variation in melting behavior of polymer–diluent systems with crystallization temperature and concentration can therefore be attributed to the change in crystal perfection of the semicrystalline lattice.

The $\Delta H_u$ estimated from eq 2 can be used to calculate the fraction of crystallinity, $\omega_c$, by the relation

$$\omega_c = \Delta H/\Delta H_u \qquad (3)$$

where $\Delta H$ is the experimentally obtained heat of fusion per mole of repeat unit obtained by calorimetry. X-ray diffraction is often used for the determination of $\omega_c$,[35] but it is difficult to differentiate scattering due to crystal imperfection or small crystallite size from scattering from truly amorphous regions. The $\omega_c$ determined by X-ray diffraction may be used to calculate $\Delta H_u$ via eq 3. Thus, the $\Delta H_u$ determined by the different techniques may be compared and yield useful information as to the semicrystalline structure of a polymer.

We have found no examples using the F–H equation (eq 2) to treat the depression of the crystal–nematic phase transition of a TLCP as an excess component. The ideal solution theory for the crystal–nematic phase transition has been shown to be an accurate predictor for binary mixtures of small molecules. We report here the first application of the F–H theory to a TLCP/LMWLC system. The F–H theory is based upon the entropy of mixing a flexible polymer with a small molecule diluent. The binary phase diagram for the crystal–nematic phase transition of BPE/I/N20 exhibits close agreement with eq 2. BPE/I/N20 is a semiflexible copolymer with a high concentration of "kinks" due to the isophthalate units. The heat for the crystal–nematic transition is generally >90% of the total heat of transition from the crystal to the isotropic state.[2,37] Therefore, we conclude that the F–H model can be applied to TLCP/LMWLC systems specifically for copolyesters containing flexible covalent bonds and meta substitution. These copolyesters are more similar to flexible chains than to rigid rods,[38] and indeed the agreement of the BPE/I/N20–DMELC system with eq 2 is confirming.

**Solid-State Transesterification in Polymer Systems.** Polyesters such as poly(ethylene terephthalate) (PET) are generally processed at low molecular weight (<10 000 g/mol) followed by heat treatment in the solid state at temperatures where transesterification can increase the molecular weight.[25] Residual catalysts in the polyester may aid in solid-state transesterification.

Lenz et al.[26-30] discovered a crystallization-induced reaction (CIR) that involves ester interchange reorganization of random copolymers. Blocky crystalline sequences are formed by solid-state trans reactions, preferably in the presence of a catalyst. Of particular interest are the CIR for the PET/PHB copolymers in the liquid-crystalline state.[30] It has been reported that after the CIR process, multiblock crystalline oxybenzoate sequences are formed; i.e., the polymer becomes more blocky, as evidenced by the insolubility of the oxybenzoate sequences. Calcium acetate, sodium acetate, and *p*-toluenesulfonic acid were studied as transesterification catalysts.

Kotliar[31] has reviewed interchange reactions involving condensation polymers, polyesters, and polyamides. His paper cites pertinent literature through 1980 and discusses the statistics of three different exchange reactions: intermolecular alcoholysis, intermolecular acidolysis, and transesterification. In this paper "transesterification" is used as a general term to describe all three types of ester interchange.

The novel processing technique described here includes the solid-state reaction of a bifunctional LMWLC into a TLCP. A similar reaction scheme is used in the synthesis of the PET/PHB copolyesters.[32] These copolymers are prepared by the acidolysis of PET with *p*-acetoxybenzoic

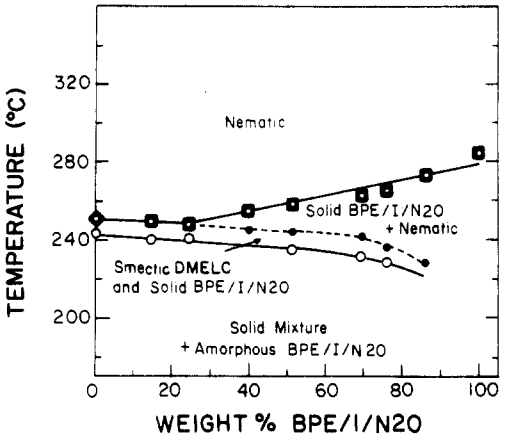


**Figure 3.** Phase diagram of BPE/I/N20–DMELC system. Heating 10 °C/min.

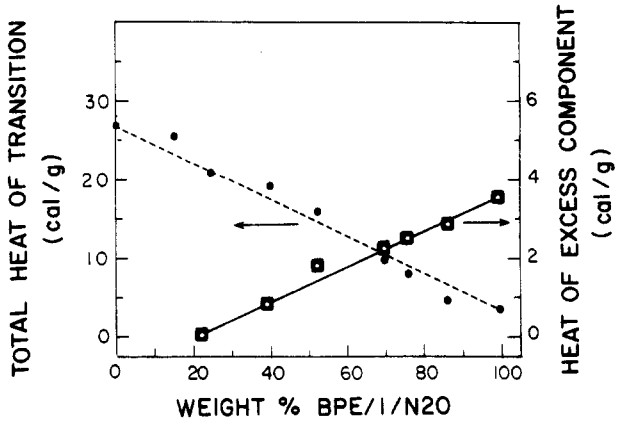


**Figure 4.** Thermal heat of transition data of BPE/I/N20–DMELC system. Heating 10 °C/min.

acid and polycondensation through the acetate and carboxyl groups. After the initial melt reaction, the copolyester was heated-treated in the solid state at 210–220 °C to increase the molecular weight. On heating, the inherent viscosity (IV) of the system is initially reduced, followed by a gradual increase of IV with reaction time at 220 °C. This corresponds to a reduction of molecular weight, a preferred reduction in viscosity for processing. For the case of the novel processing technique, a LMWLC such as DMELC is utilized in the nematic phase for processing followed by solid-state transesterification in the processed material.

The analogies between the synthesis of the PET/PHB copolyesters and the reaction of BPE/I/N20–DMELC were investigated and reported here. The reaction of the blends was studied as a function of the initial polymer molecular weight, reaction time at 220 °C, and concentration.

## Experimental Section

Phase transitions and transition heats were measured on a Perkin-Elmer DSC-2 differential scanning calorimeter and by a Zeiss polarizing microscope equipped with a Koffler hot stage monitored by a Valley Forge variable temperature programmer. All measurements were taken at heating and cooling rates of 10 °C/min. The DSC peak maxima correspond well with the temperature of the predominant change observed in the microscope (±1 °C).

Thermogravimetric analyses were performed with a Perkin-Elmer TGS-2 equipped with a System 4 microprocessor controller. All measurements were made at a heating rate of 10 °C/min with a nitrogen gas flow of 40 $cm^3$/min. Sample weights were 3–5 mg.

The binary mixtures for phase-diagram studies were prepared by refluxing for 4 h in a 60/40 phenol–1,1,2,2-tetrachloroethane solvent followed by coprecipitation into methanol. The coprecipitate was filtered, rinsed with warm methanol, and refluxed in methanol an additional 5 h. The coprecipitate was again rinsed with warm methanol and dried in vacuo at 100 °C for 48 h.

Inherent viscosity ($\eta_{inh}$) measurements were made with a Cannon-Ubbelohde viscometer at 25 ± 0.01 °C at a concentration of 0.1 g/$cm^3$ in the 60/40 phenol–1,1,2,2-tetrachloroethane solvent.

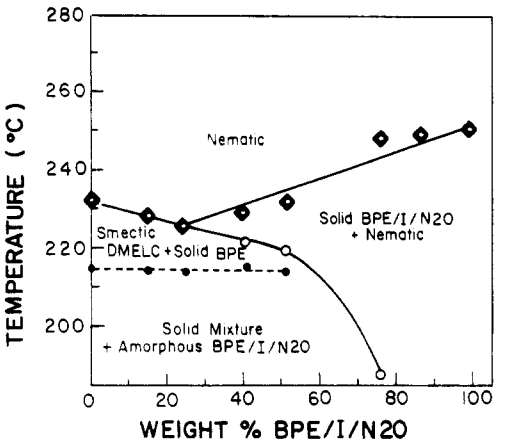


**Figure 5.** Phase diagram of BPE/I/N20–DMELC system. Cooling 10 °C/min.

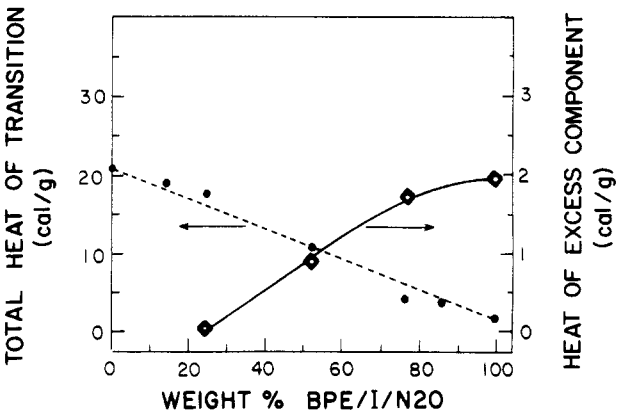


**Figure 6.** Thermal heat of transition data of BPE/I/N20–DMELC system. Cooling 10 °C/min.

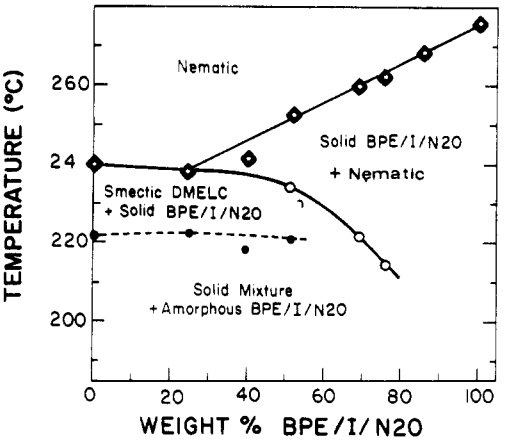


**Figure 7.** Phase diagram of BPE/I/N20–DMELC system (second heating 10 °C/min).

## Results and Discussion

**Phase Diagrams and Heat of Transition.** The isobaric phase diagrams and the associated transition heats are shown in Figures 3–8 for the system poly(bisphenol E isophthalate-*co*-naphthalate)/bis(*p*-(methoxycarbonyl)-phenyl) terephthalate. The polymer was synthesized with

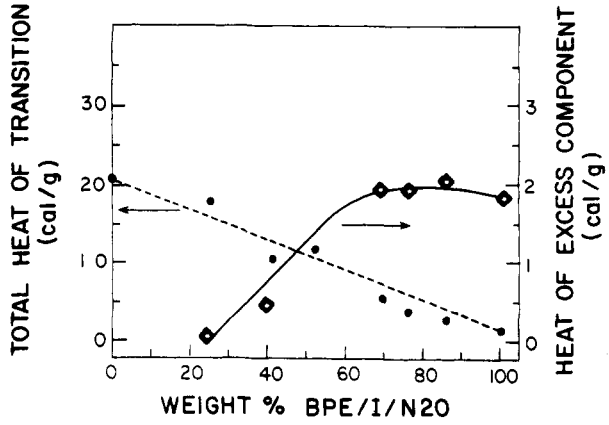


**Figure 8.** Thermal heat of transition data of BPE/I/N20–DMELC system (second heating 10 °C/min).

a 20% acid equivalent of the naphthalenedicarboxylic acid. Phase-diagram points were plotted as the peak maxima from DSC. The phase diagrams are not at equilibrium but are representative of real processing conditions. Each phase diagram exhibits eutectic-type behavior for the temperature and transition heats into a miscible nematic phase. The transition heats for the polymer as the excess component tend to 0 at the eutectic (Figures 4, 6, and 8). The change is linear (see Figure 4), but on subsequent cooling and second heating (Figures 6 and 8) curvature arises. This can be attributed to the difference in crystallization conditions. The initial blends were prepared by coprecipitation, while the data in Figures 6–8 are for blends crystallized from the melt.

Each phase diagram has four major regions. The first, at lower temperatures but above the glass-transition temperature of the polymer, is a solid mixture of BPE/I/N20 crystals and DMELC crystals plus the amorphous component of the polymer. At a higher temperature the crystal DMELC changes to a smectic liquid crystal. Under equilibrium conditions the boundary between two three-phase regions must be a horizontal line. The curvature observed in Figure 3 can be attributed to the polydispersity of molecular weights of the polymer.[40] Figures 5 and 7 exhibit an approximate horizontal straight line between the two three-phase regions but only below 52 wt % polymer. Above 52 wt % polymer significant supercoolings of the third region were observed in Figure 5, and upon second heating Figure 7 resembles the phase behavior of Figure 5. The crystal–smectic transition was not observed in this region of the phase diagram. The copolyester is expected to alter the phase behavior of DMELC, particularly at higher copolyester concentrations.

The third region of phase diagrams consists of solid crystals of BPE/I/N20 and amorphous regions plus a nematic phase. This three-phase region crosses a curve into a miscible nematic phase. This curve can be predicted by eq 2. The amorphous phase of the polymer above the glass-transition temperature may be nematiclike but tied together by the crystalline phase. It is not expected to be truly nematic until the crystals melt into the nematic phase.

The copolyester BPE/I/N20 has a low degree of crystallinity, and its eutectic melting in blends, where DMELC is in excess (<24 wt %), cannot be distinguished from the crystal–smectic transition of DMELC. In this region these two transitions are plotted as coincident. Figure 9 illustrates these DSC thermograms at low polymer concentration, and the eutectic melting is evidenced by a slight broadening of the phase transition near the crystal–smectic peak. Several DSC thermograms and a detailed analysis

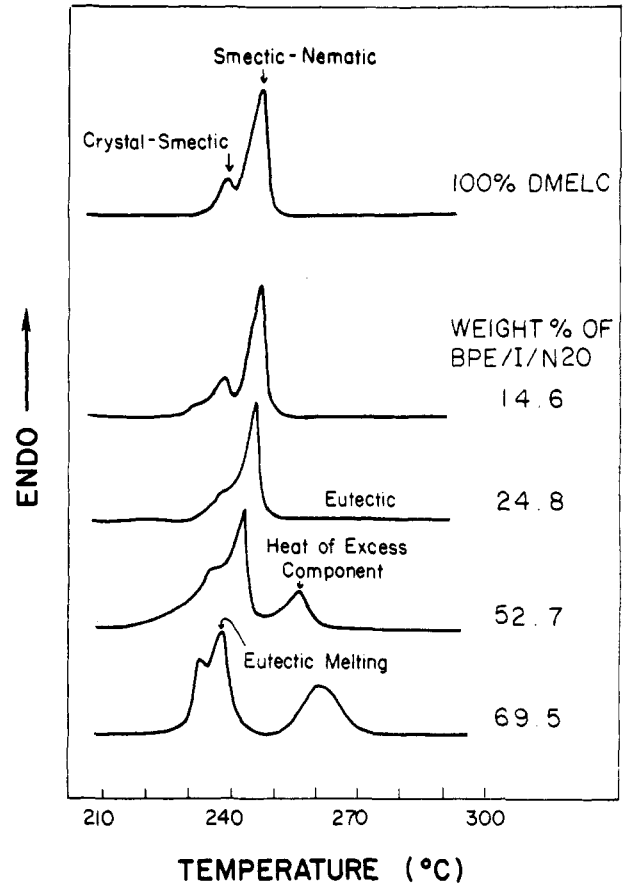


**Figure 9.** DSC thermograms of BPE/I/N20 blends with DMELC.

**Table I**
**Properties for Binary Liquid-Crystal Components**

| | density, g/cm$^3$ | molar volume, cm$^3$/mru[a] | MW | MW/ mru[a] |
|---|---|---|---|---|
| BPE/I/N20 | 1.30 | 264.0 | ~10 000[b] | 344 |
| DMELC | ~1.1 | 394.0 | 434 | 434 |

[a] Mole of repeat unit. [b] Estimated from inherent viscosity.

of DMELC have been previously presented.[2] Polarized optical microscopy for these compositions shows a crystal–smectic transition of the DMELC component followed by a simultaneous transition of the smectic–BPE/I/N20 mixture to a mixed nematic mesophase with a nematic Schlieren texture.

Transesterification is possible in this binary phase diagram and contributes to the nonideal nature of the phase diagrams, particularly in Figures 5 and 7.

**Flory–Huggins Theory for Transition Point Depression.** The lowering of the crystal–nematic transition of the polymer repeat unit in the crystal as a function of the composition in the mesophase is found to be expressed quantitatively by eq 2. $T_m$ is the maximum temperature at which crystalline regions may coexist with a mesophase and is measured experimentally. $T_{m_0}$ is the equilibrium melting temperature of a theoretical perfect crystal of the copolyester. The value used for all calculations was that for the as-prepared sample. The copolyester was initially prepared as a prepolymer followed by heat treatment to increase the molecular weight by solid-state transesterification.[39] Since these temperatures correspond to annealing conditions, the as-prepared polymer has a melting point approaching that of the equilibrium melting temperature.[24] The value for the molar volume, $V_u$, is for the polymer in the mesophase. Therefore, the density

**Table II**
**Crystal–Nematic Temperature and Compositions for the Binary System BPE/I/N20–DMELC**

| BPE/I/N20, wt % | $\phi_1$[a] | $1/T_m \times 10^3$ | $T_m$ | $[(1/T_m - 1/T_{m0})/\phi_1] \times 10^4$ |
|---|---|---|---|---|
| 86.4 | 0.153 | 1.826 | 547.6 | 1.56 |
| 76.1 | 0.271 | 1.866 | 536.0 | 2.36 |
| 69.5 | 0.341 | 1.870 | 534.9 | 1.99 |
| 52.7 | 0.515 | 1.89 | 529.1 | 1.74 |

[a] Volume fraction of DMELC.

value used for the calculation of $V_u$ was that for a quenched BPE/I/N20 sample, since this value should approach its mesophase density.

The material constants for the pure components of the phase diagram (Figure 3) are presented in Table I. The density of BPE/I/N20 was measured by a density gradient method, and the density of DMELC was estimated from that of homologous compounds.[36] The inherent viscosity of BPE/I/N20 used in the phase diagrams was 1.0 dL/g. The Mark–Houwink exponent is ~0.98 for a series of homologous thermotropic liquid crystal polymers.[1] We estimated the molecular weight to be ~10 000 g/mol on the basis of the inherent viscosity and exponent values.

Assuming that 10 000 is of sufficient molecular weight to apply eq 2, we applied the F–H theory for transition temperature depression for the data presented in Table II. This depression data is for the crystal–nematic phase transition. From eq 2, $\Delta H_u$ was calculated as 20.3 cal/g or 7.04 kcal/mol of repeat unit. BPE/I/N20 was shown to have a random sequence of termonomer units,[3,4] and the calculations based on a repeat unit assume that all units crystallize and also form the mesophase. This calculation accounts for the heat of fusion for the crystal–nematic transition and does not account for the entire heat of fusion to an isotropic state. However, the heat of the crystal–nematic transition is generally greater than 90% of the heat of fusion from the crystal to the isotropic phase.[2,37]

Simoff and Porter[4] reported the degree of crystallinity for BPE/I/N20 which exhibited a $\Delta H$ (heat of the crystal–nematic phase transition measured by DSC) of 5.5 cal/g to be ~24% by X-ray diffraction. Based on eq 3, the $\Delta H_u$ for BPE/I/N20 was 22.9 cal/g or 7.64 kcal/mol of repeat unit. The percent crystallinity calculated from X-ray diffraction is determined by separating amorphous from crystalline scattering.

The values of $\Delta H_u$ for other polyesters range from 3 to 12 kcal/mol of repeat unit.[17,24] Rigid backbones give rise to a lower heat of fusion, since there is a limited contribution from conformational mobility at the phase transition. The values of 7.04 kcal/mol of repeat unit and 7.64 kcal/mol of repeat unit for the crystal–nematic phase transition are in reasonable agreement considering the different characterization techniques.

The calculated interaction parameter, $\chi$, was 0.04. The positive value indicates the absence of strong interactions in the binary system and that the large entropy of mixing accounts for miscibility in the nematic phase. The positive value of $\chi$ also indicates that during coprecipitation of the BPE/I/N20–DMELC cocrystallization is not favored and indeed is not observed.

The application of eq 2 for transition point depression is dependent upon two adjustable parameters, $T_{m_0}$ and $(V_u/V_1)$. It was pointed out by a referee[40] that eq 2 is accurate for the determination of $\Delta H_u$ but small variations in the adjustable parameters will yield large variations in $\chi$. The main objective of this research is the calculation and interpretation of $\Delta H_u$, and eq 2 proved to be useful for these objectives.

**Effect of Molecular Weight on Phase Behavior and Solid-State Transesterification of BPE/I/N20–DMELC.** The compositions of the unreacted blends with the corresponding temperatures and heats of transition are presented in Table III. The initial molecular weight of the pure BPE/I/N20 is found not to significantly affect the transition depression of the polymer, indicating that the crystal structure of the BPE/I/N20 does not change with molecular weight. A detailed analysis of this series for BPE/I/N20 copolyesters was reported by Simoff and Porter.[2,3]

The most significant change in the binary-phase behavior of these unreacted blends is that all transition heats increase with decreasing molecular weight of the BPE/I/N20. This can be attributed to a decrease in the crystallization rate with increasing molecular weight of the polymer. It is well-known that the diffusion and the viscosity of polymers depend upon molecular weight. The crystallization of the eutectic requires the mutual diffusion of polymer segments and solvent segments, which is enhanced as the molecular weight of the polymer decreased, as indicated by the larger transition heats in Table III.

The compositions of Table III were caused to react at 220 °C in vacuo. Two similar binary compositions for each of the polymer molecular weights were studied to compare the possible effects of end-group concentration on transesterification. The polymer with an $\eta_{inh}$ of ~1.00 dL/g contained an experimental catalyst consistent with its higher $\eta_{inh}$. The polymers with an $\eta_{inh}$ of 0.67 and 0.43 contained no transesterification catalysts during the initial polymerization.

The transition heats and temperatures resulting from reaction are shown in Table IV. Representative DSC thermograms, as a function of reaction time, are illustrated in Figures 10–12 for the ~75 wt % composition for each initial molecular weight of BPE/I/N20. The reaction temperature of 220 °C is an effective annealing tempera-

**Table III**
**Temperatures and Heats of Transition for Unreacted Blends and Pure Components**

| $\eta_{inh}$ of pure BPE/I/N20 | wt % BPE/I/N20 in DMELC | $T_g$,[a] K | $T_1$,[b] K | $\Delta H_1$, cal/g | $T_2$,[c] K | $\Delta H_2$, cal/g | $\Delta H_{tot}$, cal/g |
|---|---|---|---|---|---|---|---|
| 1.0 | 100 | 400 | | | 555 | | 3.6 |
| 1.0 | 86 | 400 | 504 | 2.1 | 544 | 2.7 | 4.4 |
| 1.0 | 76 | 400 | 508 | 5.3 | 536 | 2.4 | 7.7 |
| 0.67 | 100 | 388 | | | 555 | | 3.8 |
| 0.67 | 84 | 387 | 499 | 3.8 | 545 | 4.7 | 8.5 |
| 0.67 | 75 | 390 | 509 | 6.7 | 540 | 3.7 | 10.3 |
| 0.43 | 100 | 390 | | | 555 | | 3.9 |
| 0.43 | 85 | 385 | 496 | 3.6 | 540 | 5.2 | 8.9 |
| 0.43 | 75 | 390 | 507 | 7.8 | 536 | 4.7 | 12.5 |

[a] Glass-transition temperature estimated by DSC (10 °C/min). [b] $T_1$ and $\Delta H_1$: temperature and heat of transition of the eutectic plus crystal–smectic phase transition. [c] $T_2$ and $\Delta H_2$: temperature and heat of transition of the crystal–nematic phase transition for excess BPE/I/N20.

**Table IV**
**Temperature and Heat of Transition Data for Transreacted Binary Blends (220 °C)**

| reaction time, h | $\eta_{inh}$, pure polymer | wt % BPE/I/N20 in DMELC | $T_g$, K | $T_1$, K | $\Delta H_1$, cal/g | $T_2$, K | $\Delta H_2$, cal/g | $\Delta H_{tot}$, cal/g |
|---|---|---|---|---|---|---|---|---|
| 3 | 1.0 | 76 | ~370 | | | 509 | 3.3 | 3.3 |
| 5 | 1.0 | 76 | 400 | | | 555 | 3.4 | 3.4 |
| 1.5 | 1.0 | 86 | | 480 | 1.4 | 552 | 2.2 | 3.6 |
| 5 | 1.0 | 86 | | 491 | 1.1 | 555 | 2.9 | 4.0 |
| 3 | 0.67 | 75 | 380 | 502 | 8.9 | 549 | 0.4 | 9.3 |
| 5 | 0.67 | 75 | 380 | 492 | 3.0 | 548 | 0.5 | 3.5 |
| 3 | 0.67 | 84 | 375 | 494 | 6.2 | 534 | 3.7 | 9.9 |
| 5 | 0.67 | 84 | 375 | 479 | 1.9 | 519 | 3.2 | 5.1 |
| 3 | 0.43 | 75 | | 504 | | ~520 | | 8.2 |
| 5 | 0.43 | 75 | | 505 | | ~519 | | 8.9 |
| 3 | 0.43 | 85 | 360 | 485 | 2.0 | 518 | 2.4 | 4.4 |
| 5 | 0.43 | 85 | 370 | 434 | 1.9 | 517 | 3.9 | 5.8 |

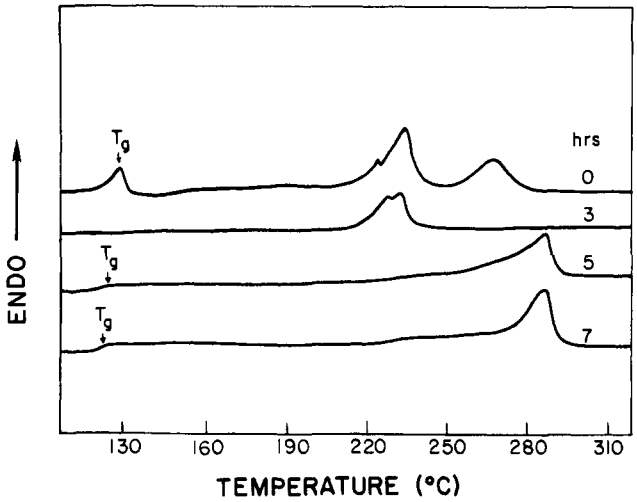


**Figure 10.** DSC thermograms for 76 wt % BPE/I/N20–DMELC reacted at 220 °C. Initial $\eta_{inh}$ of BPE/I/N20 = 1.0.

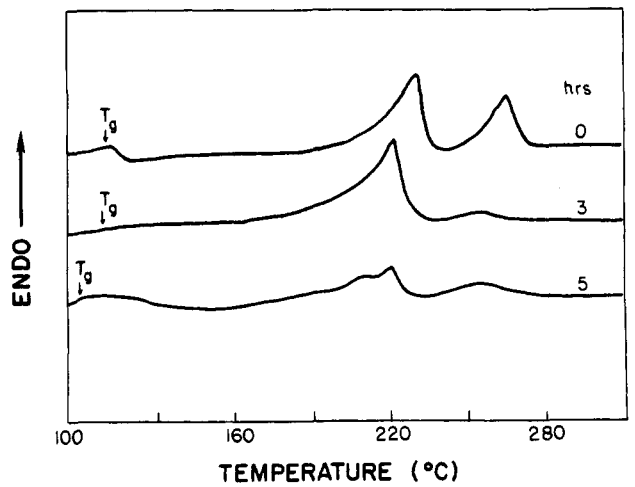


**Figure 11.** DSC thermograms for 75 wt % BPE/I/N20–DMELC reacted at 220 °C. Initial $\eta_{inh}$ of BPE/I/N20 = 0.67.

ture. DMELC contains PHB units which may undergo a crystallization-induced reaction as cited earlier. Longer sequences of PHB are expected to exhibit higher transition points and insolubility.

The DSC thermograms for the polymer containing an experimental catalyst (Figure 10) exhibited different properties than those for the systems with no catalyst (Figures 11 and 12). After 3 h at 220 °C there is observed only one peak at ~236 °C and no $T_g$ can be detected. The $T_g$ in the unreacted blend is pronounced due to enthalpy

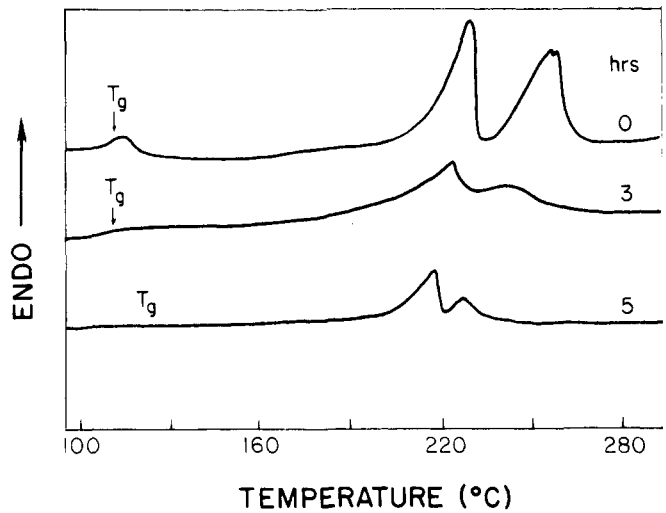


**Figure 12.** DSC thermograms for 76 wt % BPE/I/N20–DMELC reacted at 220 °C. Initial $\eta_{inh}$ of BPE/I/N20 = 0.43.

**Table V**
**Temperature of First 5 wt % Loss by TGA**

| blend reaction time, h, at 220 °C | wt % BPE/I/N20 in DMELC | $\eta_{inh}$, pure polymer | $\eta_{inh}$, blend | temp, °C, 5 wt % loss |
|---|---|---|---|---|
| | 100 | 1.0 | 1.0 | 425 |
| | 0 (DMELC) | | | 291 |
| 0 | 76 | 1.0 | 0.75 | 330 |
| 5 | 76 | 1.0 | insoluble | 455 |
| | 100 | 0.43 | 0.43 | 375 |
| 0 | 75 | 0.43 | 0.34 | 332 |
| 3 | 75 | 0.43 | 0.25 | 337 |
| 5 | 75 | 0.43 | 0.30 | 343 |

recovery and subsequent cold crystallization. After 5 h the transition temperature increased to 282 °C, equivalent to the original BPE/I/N20 and $T_g$ is observed at ~127 °C. This trend in transition behavior with reaction time is attributed to an initial reduction of molecular weight, followed by a random transesterification reaction that rebuilds the molecular weight, but with a higher concentration of PHB units and terephthalate units characteristic of DMELC. The reaction for this blend has been investigated by TGA[1] with the results in Table V.

The reaction of the 76 wt % blend containing a transesterification catalyst was also confirmed by X-ray diffraction analysis. Crystalline DMELC exhibits three distinct low-angle reflections corresponding to *d*-spacings of 24, 12, and 8 Å.[2] These reflections are clearly present in diffraction from the unreacted blend, but after reaction

**Table VI**
**Inherent Viscosities[a] for Reacted Blends of BPE/I/N20 DMELC**

| blend reaction time, h, at 220 °C | wt % BPE/I/N20 in DMELC | $\eta_{inh}$, pure polymer | $\eta_{inh}$, blend |
|---|---|---|---|
| 0 | 75 | 0.67 | 0.51 |
| 3 | 75 | | 0.16 |
| 5 | 75 | | 0.36 |
| 0 | 84 | 0.67 | 0.58 |
| 3 | 84 | | 0.22 |
| 5 | 84 | | 0.38 |
| 0 | 75 | 0.43 | 0.34 |
| 3 | 75 | | 0.25 |
| 5 | 75 | | 0.30 |
| 0 | 85 | 0.43 | 0.37 |
| 3 | 85 | | 0.68 |
| 5 | 85 | | 0.47 |

[a] $\eta_{inh}$ measured at 25 °C at a concentration of 0.1 g/cm$^3$ in 60/40 phenol–1,1,2,2-tetrachloroethane solvent.

at 220 °C for 5 h, these low-angle reflections are no longer observable.

The characteristic feature of all the blends with reaction time (Table IV) is that the heat of eutectic transition decreases, and for the 76 wt % blend with transesterification catalyst, the eutectic was not observed. Reaction in the binary blends would necessarily remove the low molecular weight DMELC, and the $\Delta H$ of the eutectic decreases. For the polymers with initial $\eta_{inh}$ of 0.67 and 0.43, no catalyst was present, and the corresponding reactions were slower. The transition heat of the excess component (BPE/I/N20) increased with reaction time in all cases except the 84 wt % blend containing BPE/I/N20 with an initial $\eta_{inh}$ of 0.67. This trend is evidence for reaction and possibly a CIR where longer sequences of PHB rearrange in the crystalline portion of the semicrystalline structure.

The crystal–nematic transition temperature, $T_2$, of the excess component decreases with reaction time for the uncatalyzed systems. DMELC contains a nonstoichiometric equivalent of hydroxyl to acid functionality: a decrease of molecular weight is thus expected with reaction time. Table VI illustrates that the $\eta_{inh}$ decreased with reaction time in all cases except for the 85 wt % blend containing an initial BPE/I/N20 $\eta_{inh}$ = 0.43, where an initial increase of $\eta_{inh}$ was observed. This can be attributed to reactions at end groups of the polymer chains, followed by random transesterification where a decrease of $\eta_{inh}$ was observed.

The BPE/I/N20 polymer contains 40% meta-substituted isophthalate units. The reaction with DMELC decreases the molecular weight but increases the overall amount of para substitution in the polymer. This change in structure will subsequently change the hydrodynamics and increase the Mark–Houwink exponent. The increase in para substitution from reaction with DMELC is also consistent with TGA results in Table V. Foti et al. investigated the properties of polyesters by pyrolysis–mass spectrometry (P–MS).[33,34] The temperature of degradation increased with the degree of para substitution.

Table V reports the temperature at which a 5 wt % loss was observed at a heating rate of 10 °C/min in a nitrogen atmosphere. This temperature is reported for the two pure components and for two representative blends as a function of reaction time. The polymer with a lower $\eta_{inh}$ (0.43) exhibited a much lower temperature for 5 wt % loss than that of the polymer with an $\eta_{inh}$ of 1.0. This can be attributed to the polydispersity nature with more lower molecular weight fragments in the polymer with $\eta_{inh}$ = 0.43. The degradation tempertures for the two unreacted blends are essentially identical (330 and 332 °C), but after reaction, the degradation temperature increased for both blends but significantly more for the polymer containing a transesterification catalyst. This can be attributed to a more complete reaction in the presence of the catalysts, producing longer sequences of PHB units. These TGA results also confirm the slow rate of the transesterification reaction.

The reaction of BPE/I/N20–DMELC in the solid state was unambiguously proved by the data from DSC, TGA, X-ray diffraction, and dilute-solution viscosity. The presence of a suitable catalyst reduces processing times for production of more rigid, more thermally stable polymers via the novel approach for processing thermotropic liquid-crystalline polymers.

**Acknowledgment.** We thank Oliver Deex of Monsanto for supplying the copolyester used in this investigation and also A. C. Griffin of the University of Southern Mississippi for synthesizing the DMELC.

## References and Notes

(1) Calundann, G. W.; Jaffe, M., presented at the Robert A. Welch Conference on Chemical Research, Houston, TX, Nov 15–17, 1982.
(2) George, E. R.; Porter, R. S.; Griffin, A. C. *Mol. Cryst. Liq. Cryst.* **1984**, *110*, 27.
(3) Simoff, D. A. Masters Thesis, University of Massachusetts, 1983.
(4) Simoff, D. A.; Porter, R. S. *Mol. Cryst. Liq. Cryst.* **1984**, *110*, 1.
(5) Hsu, E. C. H.; Johnson, J. F. *Mol. Cryst. Liq. Cryst.* **1973**, *20*, 177.
(6) Hsu, E. C. H.; Johnson, J. F. *Mol. Cryst. Liq. Cryst.* **1974**, *25*, 145.
(7) Demus, D.; Fietkau, C. H.; Schubert, R.; Kehlen, H. *Mol. Cryst. Liq. Cryst.* **1974**, *25*, 215.
(8) Griffen, C. W.; Porter, R. S. *Mol. Cryst. Liq. Cryst.* **1973**, *21*, 77.
(9) Albert, W.; Haim, E.; Yee, D. *Mol. Cryst. Liq. Cryst.* **1979**, *51*, 67.
(10) Griffin, A. C.; Havens, S. J. *J. Polym. Sci., Polym. Lett. Ed.* **1980**, *18*, 259.
(11) Cser, F.; Nyitrai, K.; Hardy, Gy. *J. Polym. Sci., Polym. Symp.* **1977**, *61*, 9.
(12) Finkelmann, H.; Kock, H. J.; Rehage, G. *Mol. Cryst. Liq. Cryst.* **1982**, *89*, 23.
(13) Millaud, B.; Thierry, A.; Skoulios, H. *Mol. Cryst. Liq. Cryst.* **1978**, *41*, 263.
(14) Noël, C.; Billard, J. *Mol. Cryst. Liq. Cryst.* **1978**, *41*, 269.
(15) Billard, J.; Blumstein, A.; Vilasagar, S. *Mol. Cryst. Liq. Cryst.* **1982**, *72*, 163.
(16) Fayolle, B.; Noël, C.; Billard, J. *J. Phys. Colloq.* **1979**, *40*, C3-485.
(17) Flory, P. J. "Principles of Polymer Chemistry"; Cornell University Press: Ithaca, NY, 1953; p 568.
(18) Scatchard, G. *Chem. Rev.* **1931**, *8*, 321.
(19) Hildebrand, J. *J. Am. Chem. Soc.* **1916**, *38*, 1452. *Ibid.* **1919**, *41*, 1067. *Ibid.* **1920**, *42*, 2180.
(20) Smith, P.; Pennings, A. J. *Polymer* **1974**, *15*, 413.
(21) Smith, P.; Pennings, A. J. *J. Mater Sci.* **1976**, 1450.
(22) Gryte, C. *J. Polym. Sci., Polym. Phys. Ed.* **1979**, *17*, 1295.
(23) Vasanthakumari, R. *Polymer* **1981**, *22*, 862.
(24) Wunderlich, B. "Macromolecular Physics"; 1979; Vol. 3, p 107.
(25) Prevorsek, D. "Polymer Liquid Crystals"; Ciferri, A.; Krigbaum, W. R.; Meyer, R. B., Eds.; Academic Press: New York, 1982; p 334.
(26) Lenz, R. W.; Miller, W. R.; Pryde, E. H.; Awl, R. A. *J. Polym. Sci., Polym. Chem. Ed.* **1970**, 8, 429.
(27) Lenz, R. W.; Go, S. *J. Polym. Sci., Polym. Chem. Ed.* **1973**, *11*, 2927.
(28) Lenz, R. W.; Go, S. *J. Polym. Sci., Polym. Chem. Ed.* **1974**, *12*, 1.
(29) Lenz, R. W.; Schuler, A. N. *J. Polym. Sci., Polym. Symp.* **1978**, *63*, 343.
(30) Lenz, R. W.; Jin, J. I.; Feichtinger, K. A. *Polymer* **1983**, *24*, 327.
(31) Kotliar, A. M. *Macromol. Rev.* **1981**, *16*, 367.
(32) Jackson, W. J., Jr.; Kuhfuss, H. F. *J. Polym. Sci., Polym. Chem. Ed.* **1976**, *14*, 2043.

(33) Foti, S.; Giuoffrida, M.; Maravigna, P.; Montaudo, G. *Polym. Prepr. (Am. Chem. Soc., Div. Polym. Chem.)* **1984**, *25*, 88.
(34) Foti, S.; Montaudo, G. "Analysis of Polymer Systems"; Burk, L. S.; Allen, N. S., Eds.; Applied Science: London, 1982.
(35) Alexander, L. E. "X-Ray Diffraction Methods in Polymer Science"; Wiley-Interscience: New York, 1969.
(36) Dewar, M. J. S.; Goldberg, R. S. *J. Org. Chem.* **1970**, *35*, 2711.
(37) Johnson, J. F.; Porter, R. S.; Barrall, E. M., II, *Mol. Cryst. Liq. Cryst.* **1969**, *8*, 1.
(38) Flory, P. J. *Proc. R. Soc. London, Ser. A* **1956**, *234*, 73.
(39) Deex, O. D. Weiss, V. W. U.S. Patent 4 102 864, 1978, (Monsanto).
(40) Koningsveld, R., private communication, University of Massachusetts, 1985.

# Dynamics of Entangled Linear, Branched, and Cyclic Polymers

**Jacob Klein**

*Polymer Research,† Weizmann Institute of Science, Rehovot 76 100, Israel, and Cavendish Laboratory, Madingley Road, Cambridge, England.* *Received April 4, 1985*

ABSTRACT: We evaluate the translational diffusion coefficients and longest relaxation times for entangled linear $n$-mers, for $f$-arm star branched polymers ($n_b$-mers/arm), and for cyclic (closed ring) polymers ($n_R$-mers) in a fixed entanglement network and also in a melt of entangled linear $p$-mers. "Tube-renewal" effects for the latter case are reexamined, taking into account both hydrodynamic interactions and especially the interdependence of $p$-mer constraints about a diffusing $n$-mer; the characteristic tube-renewal time in this case becomes $\tau_{tube} \sim n^2p^{5/2}$, in contrast with earlier proposals. At very high $n$ values one expects an unscreened form for the tube-renewal time, $\tau_{tube} \sim n^{3/2}p^3$, equivalent to the "hydrodynamic sphere" diffusion of the $n$-mer in the $p$-mer melt. The diffusion coefficients and longest relaxation times for stars in a fixed entanglement lattice are calculated with a diffusion equation approach as $D_s \sim n_b^{-1} \exp(-\alpha n_b/n_c)$ and $\tau_s \sim n_b \exp(\alpha n_b/n_c)$, with $\alpha$ a constant and $n_c$ the entanglement degree of polymerization, a form similar (in the dominant exponential term) to earlier calculations. For rings the corresponding expressions are $D_R \sim \exp(-\beta n_R/n_c)$ and $\tau_R \sim \exp(\beta n_R/n_c)$, where $\beta \gtrsim \alpha$, though these are limiting forms valid for high $n_R$ ($\gtrsim 20n_c$); at lower $n_R$ values ring polymers may exhibit a quasi-linear behavior. When incorporated in melts of linear $p$-mers, the diffusion and relaxation of both stars and rings is dominated—for $n_b$ and $n_R$ greater than some crossover value of order $10n_c$—by tube-renewal effects mediated by reptation of the linear melt matrix.

## I. Introduction

The essential topological constraint on a polymer molecule in an entangled solution or melt is that it may not pass through adjacent segments. The replacement of this condition by confining the motion of any given molecule to a "tube" defined by entanglements with its neighbors has proved to be a fruitful approximation;[1,2] for the case of linear polymers the resulting translational diffusion of the molecules (and the slowest relaxation processes) takes place by reptation, and this concept forms the basis of current molecular theories of viscoelasticity.[3-6] Although viscoelastic measurements are straightforward to carry out and reasonable (but not complete) agreement with theory has been observed,[6] translational diffusion studies may provide a more direct test of the reptation approximation. Several independent approaches, including IR microdensitometry,[7] optical techniques,[8,9] NMR[10,11] methods, and neutron[12] and nuclear scattering techniques,[13,14] as well as computer simulation studies,[15] have confirmed[16] that the translational diffusion coefficient $D(n)$ of entangled linear $n$-mers varies as

$$D(n) \propto n^{-2} \tag{I.1}$$

in agreement with the reptation prediction.[2,3] Strictly speaking, eq I.1 should apply to reptation of a flexible chain in fixed surroundings or a fixed "tube"; for a non-cross-linked, entangled polymer solution or melt the tube itself is defined by intersections with the *mobile* neighbors of any enclosed molecule, so that it may, over a time $\tau_{tube}$, renew its configuration. It was argued, however,[5,17,18] that for the case of limitingly long linear molecules one would have $\tau_{tube} \gg \tau_{rep}$, the time for a molecule to renew its configuration by reptation, so that tube-renewal effects would be unimportant in entangled linear systems of sufficiently high $n$. More direct support[14,19] for the weakness of tube-renewal effects in such systems has come from diffusion studies of a linear $n$-mer in a series of chemically identical $p$-mer melts, which showed $D(n)$ to be independent of $p$ (for $p \gtrsim 3p_c$, $p_c$ being the critical length for onset of entanglements). There have also been theoretical modifications to the concept of "fixed tubes", based on the idea of constraint release as entangling molecules diffuse away.[5,17,18] These modifications do not in general change the original power-law predictions of the reptation model in the limit of high $n$ (e.g., eq I.1) in systems of linear homopolymers.

Considerably less is known, both theoretically and experimentally, for the case of entangled *nonlinear* molecules, such as star-branched or cyclic polymers. For such molecules reptation is expected to be severely suppressed,[20] and "tube renewal" may come to dominate the longest relaxation processes. For this reason, studies of the diffusion or relaxation of *nonlinear* molecules in an entangled *linear* matrix may give more direct information on tube-renewal processes than a corresponding study in a fully linear system.

A number of treatments of the diffusion and relaxation mechanisms of entangled star-branched polymers have been given. The essential idea was first presented by de Gennes,[20] who considered the motion of a symmetric $f$-arm star with $n_b$ monomers/arm, moving in a fixed lattice of noncrossable obstacles. We shall frequently find it convenient to work in terms of

$$N = n/n_c \qquad (\text{or } N_b = n_b/n_c)$$

the mean number of entanglement lengths or primitive

† Mailing address: Polymer Research Department, Weizmann Institute of Science, Rehovot 76 100, Israel.

0024-9297/86/2219-0105$01.50/0 